Cai *et al. Environmental Sciences Europe* (2022) 34:38
https://doi.org/10.1186/s12302-022-00615-1

Environmental Sciences Europe

RESEARCH Open Access

Quantitative delimitation of radiant belt toward lake of lake-terrestrial ecotone

Tian-yi Cai†, Chun Ye*, Chun-hua Li*, Fan Zhang† and Wei-wei Wei

Abstract

Background: Lake-terrestrial ecotone is a transition zone between terrestrial and aquatic ecosystems. Linking land and lake, it is thus highly sensitive and vulnerable to disturbances. It includes three parts, namely, radiant belt toward land, shoreline zone and radiant belt toward lake. Extending from multi-year average low water level line to open water, radiant belt toward lake is a key part of lake-terrestrial ecotone. However, the delimitation method for radiant belt toward is unsolved, which is a big obstacle to protecting lake-terrestrial ecotone effectively. Wave is a major hydrodynamic factor in lakes, especially large shallow lakes. For linking landward and waterward directions, the boundary of radiant belt toward lake may be affected by waves. Hence, exampled as Lake Taihu, this research was carried out from wave perspective.

Results: In July 2021, a total of 12 species aquatic macrophyte were collected, including 3 species of floating-leaved and 9 submerged macrophyte within radiant belt toward lake of Lake Taihu. Aquatic macrophyte were incorporated into calibrated wave models driven by constant winds via MIKE21 SW. Wave height attenuation was successfully simulated, ranging − 0.19% ~ 8.89% under eastern-wind condition and − 0.08% ~ 23.37% under western-wind condition. In general, wave height gradually attenuates from shore to water. The abrupt change point in relative wave height was used as the boundary of the radiant belt toward lake. A total of 26 sampling lines from bank to water around the whole lake of Lake Taihu were set, ranging 701 ~ 2155 m. Based on the setups of sampling lines, the delimitation range of Lake Taihu is about 1 ~ 2 km.

Conclusions: A novel approach was developed for quantitative delimitation of radiant belt toward lake. Both wind forcing and aquatic vegetation has slight impact on results of delimitation, indicating the feasibility of this approach. It determines a theoretical boundary of lake-terrestrial ecotone, which is helpful to a more precise protection and restoration of large shallow lakes. Moreover, it could provide a potential method for quantitative delimitation for large shallow lakes with similar conditions.

Keywords: Lake-terrestrial ecotone, Numerical simulation, Aquatic macrophyte, Lake Taihu

Background

Lake-terrestrial ecotone is an indispensable part of aquatic ecosystem. It has a number of ecological functions, i.e., pollutant interception and purification, improving lake biodiversity and providing habitat for wildlife. However, as the result of its special structure and geographical location, lake-terrestrial ecotone is highly vulnerable to human activities. With the rapid ecological degradation and loss of ecological functions, hence, the protection and restoration of lake-terrestrial ecotone is of extraordinary significance to healthy lakes. Radiant belt toward lake is an important part of lake-terrestrial ecotone (Fig. 1). It is a transitional zone extending from the multi-year average low water level line to open water. On one hand, it is affected by waves and currents from

*Correspondence: yechbj@163.com; 297535203@qq.com
†Tian-yi Cai and Fan Zhang contributed equally to this work
National Engineering Laboratory for Lake Pollution Control and Ecological Restoration, State Environmental Protection Key Laboratory for Lake Pollution Control, Chinese Research Academy of Environmental Sciences, Beijing 100012, China

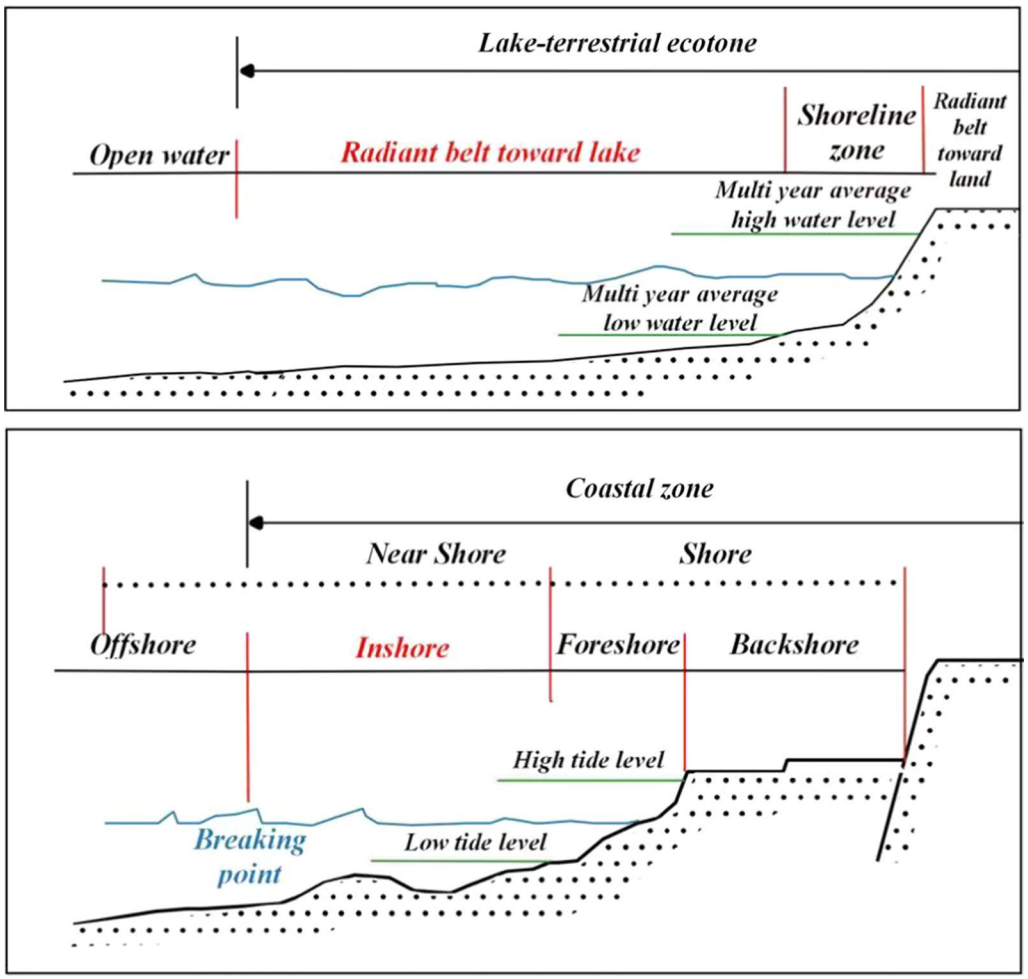

Fig. 1 Comparison of structures of lake-terrestrial ecotone and coastal zone [1]

lake, on the other hand, by land. Radiant belt toward lake is the main distribution area for floating-leaved and submerged macrophyte [1]. Ye et al. [1] had systematically and clearly defined the structure and functions of lake-terrestrial ecotone. Zheng et al. [2] delimited radiant belt toward land by moving split-window technology (MSWT) in lakes of lower Yangze River basin. In terms of prior studies in lake-terrestrial ecotone [1, 2], the quantitative delineation, especially radiant belt toward lake, still remains unclear. The lack in accurate quantitative delimitation poses a challenge to researchers and government in effective protection and restoration for lakes. Kalff [3] suggested that lake-terrestrial ecotone is the area covered or likely to be covered by aquatic macrophyte. For deep lakes, with light as the limiting factor, it is feasible to define the boundary of radiant belt toward lake as the boundary of aquatic macrophyte growth. However, simply by the disappearance of aquatic macrophyte, mostly submerged ones, it is not applicable for some large shallow lakes, i.e., Lake Taihu, for conditions of aquatic macrophyte spreading into the center of lake or no macrophyte covered in some areas [4, 5]. Thus, a new delimitation method is of urgent need to be developed to not only meet accuracy, but also to guide large shallow lakes with similar conditions. As the basis of ecological restoration for lake-terrestrial ecotone, the quantitative delineation is the primary issue for more targeted and precise control, thus it has significance in making scientific support for spatial management and ecological restoration of lakes.

With reference to coastal zone (Fig. 1), wave conditions were chosen to quantitatively delineate radiant belt toward lake of Lake Taihu, a typical large shallow lake in China. As an important hydrodynamic factor in large shallow lakes, wave conditions are vital in shaping lake basin formation and shoreline morphology [6, 7], as

well as pollutant release [8], dispersion and elimination [9]. Moreover, wave conditions are active dynamic factors within radiant belt toward lake for linking landward and waterward directions, as well [1]. The wave growth could be directly influenced by wind forcing, water depth and shoreline morphology [10], as well as aquatic macrophyte, which may lead to wave height attenuation and energy dissipation [11, 12]. At present, waves are mainly presented by empirical formulas, field observations, flume experiments and numerical simulations [13]. Numerical simulations are widely used for its high precision and low labor costs. In terms of wave numerical simulation, WAVEWATCH III, SWAN and MIKE21 SW models are mostly used. Among them, WAVEWATCH III model is mainly used in the simulation of large-scale sea area, such as the Mediterranean Sea [14], East Sea [15], Red Sea [16], and Indian Ocean [17]. SWAN and MIKE21 SW models can be used in wave simulation of nearshore and lakes, such as Black Sea [18], UK Coastal [19], Lake Taihu [20, 21]. Fonseca [22] compared the coastal spectral wave model performances, found that the grids of MIKE21 SW are better adjusted than the ones of SWAN. Hence, in this study MIKE21 SW is used to project the wave field of Lake Taihu based on the wind field information.

The aims of this study were to (i) research the distribution characteristic of aquatic macrophyte within radiant belt toward lake of Lake Taihu, (ii) simulate wave fields of Lake Taihu driven by constant winds via MIKE21 SW, (iii) incorporate aquatic macrophyte obtained by field survey into calibrated models according to definition of radiant belt toward lake, (iv) develop a delimitation method for radiant belt toward lake, (v) delimit the boundary of radiant belt toward lake of Lake Taihu, and investigate the influencing factors of the delimitation results.

Materials and methods

Study area

The study area is Lake Taihu(30° 55′ 40″–31° 32′ 58″ N, 119° 52′ 32″–120° 36′ 10″ E) in Jiangsu Province, China. It is the third largest freshwater lake in China. Lake Taihu has a current surface area of 2338.11 km^2, and a shoreline in total length is about 405 km. The average water depth is 1.9 m, and the maximum water depth is 2.6 m, Lake Taihu is a typical large shallow lake. This region has a subtropical monsoon climate with four distinct seasons, abundant rainfall and heat. The average annual precipitation of the Lake Taihu basin is 1177 mm, and the average annual temperature of Lake Taihu basin is 15–17 ℃. As the catchment center of the basin, a large amount of pollutants were carried into Lake Taihu with inflowing water, leading to a rapid decline in water quality and ecosystem degradation.

Lake Taihu has experienced a rapid ecosystem degradation since the explosive development in surrounding area. Aquatic macorphyte could reflect the health of lakes, especially ones in radiant belt toward lake. From 1960s to 2014, a total of 8 species aquatic macrophytes had disappeared, such as *Callitriche stangnalis, Utricularia minor*, the dominant species of aquatic plants show a monoculture trend, as well [23].

Field survey

In consider of the wave height attenuation that caused by aquatic macrophyte within radiant belt toward lake, a field survey was conducted in July 2021 (Additional file 1). Aquatic macrophyte were collected by a self-made sampler. The distribution of aquatic macrophyte, species, height (m), diameter (m) and density (units/m^2) were recorded in-site for further analysis and processing.

IV (important value) was used to tell the dominant species in each layer, and the aquatic macrophyte associations were named by the dominant species of each layer, respectively. The IV calculation formula, given by

$$\mathrm{IV}_1 = \left(\frac{D_1}{\sum D} + \frac{C_1}{\sum C} + \frac{F_1}{\sum F}\right) \div 3, \tag{1}$$

where IV_1 is the important value of species1 in sampling point, D_1 is the density of species1 in sampling point, $\sum D$ is the total density of vegetation in sampling point, C_1 is the coverage of species1 in sampling point, $\sum C$ is the total coverage of species1 in sampling point, F_1 is the frequency of species1 in sampling point, $\sum F$ is the total frequency in sampling point.

The aquatic macrophyte associations were named after by the dominant species in each layer, which the dominant species were determined by the IV. Same layer was connected by '+', different layer was connected by '−'.

Wave model application

MIKE21 SW introduction

MIKE21 SW spectral wave model is a third-generation wave model that simulates the growth, decay and transformation of wind-generated waves and swells in offshore and coastal areas, has been widely used [24]. It is based on the finite volume technique to solve the governing equations, taking into account the following physical phenomena: wind wave generation, refraction, shoaling, white-capping, bottom friction, wave breaking dissipation, nonlinear wave–wave and wave–current interactions [24]. Two formulations are available: directional decoupled parametric formulation and fully spectral formulation. The latter is used in this study and the governing equation is the wave action balance equation, given by

$$\frac{\partial}{\partial t}N + \frac{\partial}{\partial x}N.C_{g.x} + \frac{\partial}{\partial y}N.C_{g.y} + \frac{\partial}{\partial \theta}N.C_{\theta} + \frac{\partial}{\partial \sigma}N.C_{\sigma} = \frac{S}{\sigma} \tag{2}$$

$$S = S_{\text{in}} + S_{\text{nl4}} + S_{\text{ds}} + S_{\text{nl3}} + S_{\text{bot}} + S_{\text{surf}}. \tag{3}$$

In Eq. (2), where $N(\sigma, \theta)$ is the action density spectrum, σ is the relative radian frequency and θ is the wave direction. The first term represents the local rate of change of action density in time. The second and the third ones are action density propagation in x and y geographic spaces with propagation velocities $C_{g.x}$ and $C_{g.y}$, respectively. The fourth term is related to the depth-induced and current-induced refraction with propagation velocity C_{θ} in θ-space. The fifth term represents shifting of the relative frequency due to variations in depth and currents with propagation velocity C_{σ} in σ-space. In Eq. (3), S is the energy source term that contains a superposition of source functions which represent relevant physical phenomena. S_{in} represents the generation of wind energy, S_{nl4} is the wave energy transfer due to quadruple wave-wave interaction, S_{ds} is the dissipation of wave energy due to white-capping, S_{nl3} is the wave energy transfer due to triple wave–wave interaction, S_{bot} is the dissipation of wave energy due to bottom friction and S_{surf} is the dissipation due to depth-induced breaking.

According to definition of radiant belt toward lake, this research thus only took wind forcing as the driving force (wind speed: 5 m/s, wind direction: north, east, south, west) and bottom friction representing the presence of aquatic macrophyte into account. The bottom friction was selected as Nikuradse roughness at present research. All other parameters were set as default value according to MIKE21 SW manual [24], as well.

Model establishment and validation

For constant wind forcing, Putian Formula from "Code for design of levee project" (GB50286-2013) [25] has been proved applicable for Lake Taihu [21], in which specifies an approach to calculating wave conditions in inland lakes. Given the irregular shape of the boundary of Lake Taihu, it is necessary to introduce the equivalent fetch length for wave calculation:

$$F_e = \frac{\sum_i r_i \times \cos^2 \alpha_i}{\sum_i \cos \alpha_i}, \tag{4}$$

where r_i is the length of the ray led from the calculation point to the opposite bank at every Δ α angle within 45° on each side of the main wind direction (m), α_i is the angle between the r_i ray and the r_0 ray on the main wind direction (°). which $\alpha_i = i^* \Delta\ \alpha$, $\Delta\ \alpha = 15°$, $i = 0, \pm 1, \pm 2, \pm 3$. (Additional file 2).

Putian formula can be used to calculate average wave height and significant wave height, respectively:

$$\frac{g\overline{H}}{v^2} = 0.13 \tanh\left[0.7\left(\frac{gd}{v^2}\right)^{0.7}\right] \tanh\left\{\frac{0.0018\left(\frac{gF_e}{v^2}\right)^{0.45}}{0.13 \tanh\left[0.7\left(\frac{gd}{v^2}\right)^{0.7}\right]}\right\} \tag{5}$$

$$h_m = 1.21\overline{H}, \tag{6}$$

where g is gravity acceleration (m/s^2), $\overline{H}$ is average wave height (m), v is computational wind speed (m/s), d is the average water depth(m), F_e is equivalent fetch length (m), h_m is significant wave height (m).

To quantify computational and numerical difference of h_m, a statistical analysis and uncertainty analysis was conducted with 2 parameters: relative bias (R.bias) and root mean square error (RMSE/m), given by

$$\text{R.bias} = \frac{\left(\sum_{i=1}^{n} |s_i - m_i|\right)/n}{\overline{m}} \tag{7}$$

$$\text{RMSE} = \sqrt{\left[\sum_{i=1}^{n} (s_i - m_i)^2\right]/n}, \tag{8}$$

where s_i are values obtained by numerical simulation (m), m_i are values calculated by Putian formula (m) and n is the sample size, in present research, $n = 5$.

Numerical simulation of generalized aquatic macrophyte in MIKE21 SW

For attenuation in significant wave height that may be caused by aquatic macrophyte, the physical properties obtained from field survey were transferred into equivalent sand heights [26] with reference to aforementioned Nikuradse roughness by Manning's coefficient support [27–29] [Eqs. (9)–(11)], given by

$$n_v = \sqrt{\left(\frac{1}{M}\right)^2 + \frac{C_D m_i Dmin(h_v, h) h^{\frac{1}{3}}}{2g}} \tag{9}$$

$$K_{S_i} = \left(\frac{8.25\sqrt{g}}{n_v}\right)^6 \tag{10}$$

$$K_{s\_all} = \sum_i K_{s_i} \times \frac{m_i}{m}, \tag{11}$$

where n_v is vegetated Manning's coefficient, M is bottom Manning's coefficient, equals 50, C_D is vegetation drag coefficient, C_D equals 0,0.1,0.2,0.3 in present research, m_i is the density of the i*th* species (stems/m^2), h_v is height of vegetation (m), h is average water depth of each lake area (m), g is gravity acceleration (m/s^2), K_{si} is equivalent sand roughness height of each species(m), K_{s_all} is equivalent sand roughness height of each aquatic macrophyte association (m), i is the i*th* species of the association, K_{Si} is the ith K_S calculated by Eq. (10) (m), m is the density of the association (stems/m^2).

C_D is a crucial parameter related to hydrodynamic conditions and plant characteristics, including rigidity and submergence [30]. Flexibility and submergence of aquatic vegetation can reduce the values of C_D [31]. Previous studies proposed empirical equations in related to Reynolds number(Re) or Keulegan–Carpenter number (KC) [31]. Despite all the uncertainties and challenges posed by assessing in field. In present work constant values, $C_D=0$ and $C_D=0.1$, 0.2, 0.3 were used, with reference to Oude's research [32] (*Echinodorus grandiflorus* $C_D=0.06$–0.13, *Cabomba caroliniana* $C_D=0.07$–0.12, *Nymphaea rubra* $C_D=0.11$–0.23). In which, the $C_D=0$ represents no aquatic macrophyte on lake bed, and $C_D=0.1,0.2,0.3$ represents the different degrees in roughness caused by aquatic macrophyte on lake bed.

Wave height attenuation

To quantify the wave height attenuation caused by aquatic macrophyte incorporation, this research hereby introduce the wave height attenuation rate, given by

$$\text{Wave height attenuation rate} = \frac{(h_{m1} - h_{m2})}{h_{m1}} \times 100\%, \tag{12}$$

where h_{m1} is the significant wave height simulated, h_{m2} is the significant wave height simulated after aquatic macrophyte incorporation.

Delimit range method and sampling design

Due to the dense distribution of aquatic macrophyte in lake-terrestrial ecotone [1, 3–5] and its potential in wave height attenuation nearshore [11, 12], field survey data obtained in July 2021 were incorporated into numerical simulation in this study. Extending from multi-year average low water level line to the center of the lake [1], in total of 26 sampling lines were made perpendicular to shoreline with 500 sampling points evenly distributed (Fig. 2). In comparison of lake-terrestrial ecotone and coastal zone, it shows great similarities in profile structure. Bounded by breaking point, the sea area can be divided to offshore and coastal zone. In which, the inshore area is extending from low tide level to breaking point. The breaking point is determined by relative wave height. Hence, with reference to coastal zone [10], relative wave height (ratio of significant wave height to water depth) is selected as the indicator. The boundary of radiant belt toward lake is the end point in water area which is affected by landward according to the definition. Thus, by plotting curves between relative wave height and distance to lake shore, sampling points with abrupt change of the slope of the tangent line within curves were selected as the boundary of the radiant belt toward lake of lake-terrestrial ecotone. Since the abrupt change point whose second-order derivative is discontinuous, which is the end point of terrestrial impact on water area in mathematical expression. From wave perspective, the wave height can be influenced by wind forcing, water depth, shoreline morphology and aquatic macrophyte. In this research, the wave models were set up at certain water level. However, it is unknown that the variance of wind forcing and aquatic macrophyte would deviate the delimitation result or not due to lack of reference. To find out the boundary of radiant belt toward lake, and investigate the influencing factors of the delimitation result. The delimiting method for the boundary of radiant belt toward lake used in the present research is developed by adjusting the relative parameters, such as vegetation drag coefficients and wind directions.

Data analysis

MIKE21 SW was used to simulate the wave field of Lake Taihu. Microsoft Excel was used for data processing and analyzing, QGIS3.12 was used for plotting.

Results

Field survey

A total of 12 species aquatic macrophyte were collected in field survey in July, 2021. A total of 3 species of floating-leaved macrophyte were collected, namely, *Nymphoieds peltatum*, *N. indica* and *Trapa maximowiczii*. A total of 9 species of submerged macrophyte were collected, namely, *Potamogeton crispus*, *P. malainus*, *P. maackianus*, *Myriophyllum spicatum*, *Ceratophyllum demersum*, *Hydirlla verticillata*, *Vallisneria natans*, *Elodea nuttali* and *Najas marina*. In total of 263.06 km^2 water area was covered by aquatic macrophyte, occupying 11.25% of the total water surface area. According to the calculation of IV (Additional file 3), a total of 6 aquatic macrophyte associations were classified, respectively (Fig. 3); the composition of each macrophyte associations and the parameters obtained in field survey are listed in Additional file 4.

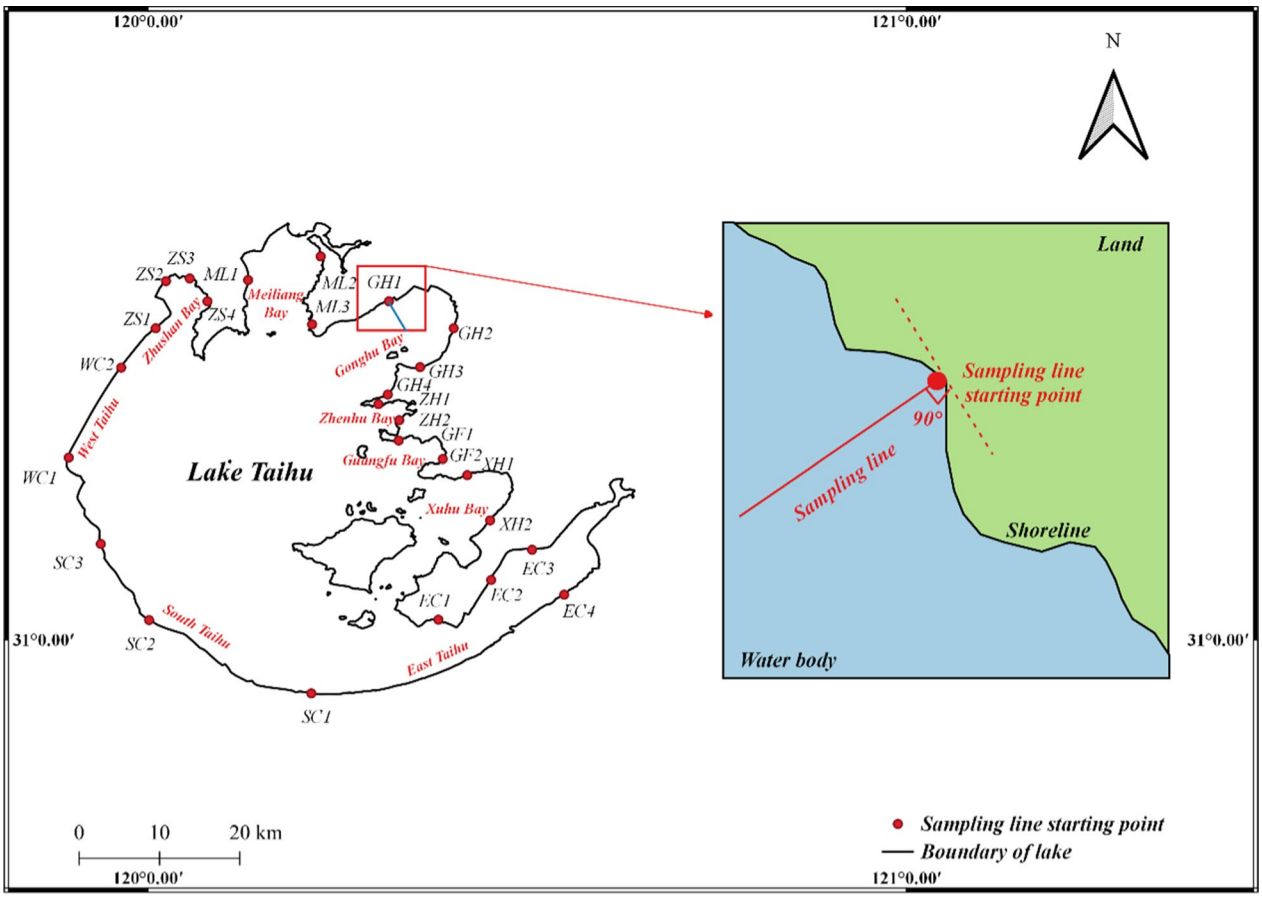

Fig. 2 Schematic of location and setup of sampling lines. In which, red dot represents the sampling line starting point, and the black line represents the boundary of lake. The right one is a scope into the setup of sampling lines, where the sampling line is made perpendicular to shoreline and extending to the lake center

Model establishment and validation

The model area is dissected using a triangular mesh of 31,611 grid cells, 16,484 grid nodes, and the grid side length is between 200 and 1000 m. Simulated by triangular mesh as a basic unit, all sides of the triangular mesh are linearly interpolated. The boundary condition is set as land boundary, constant winds are chosen as the driving force of the models. The bottom friction is selected as Nikuradse roughness, which is taken as 0.015–0.020 m. In total of 5 calibration sampling point (Additional file 5) were selected to validate the credibility of established models. The multi-year average water level of Lake Taihu, 2.99 m (Wusong Zero Datum) [33] was used in Putian formula. The computational and simulated values are listed in Table 1.

Calculated by Eqs. (7, 8), the Nikuradse roughness and the R.bias and RMSE of each model driven by different wind forcing are listed in Table 2, respectively.

Wave height attenuation caused by aquatic macrophyte

Numerical simulation of sampling lines driven by different wind directions

In this section, GH2, GH3, ZH1, ZH2, XH1, XH2, EC2, EC3 and EC4 in vegetated eastern lake areas were analyzed to investigate significant wave height simulations driven by wind from different directions. It is worth mentioning each sampling line has different lengths as a result of different scales of lake areas (Table 3).

Due to the differences in fetch length, different wind directions appear to have influence on significant wave height simulated within same sampling line. For the sampling lines selected, significant wave heights simulated driven by western wind appear to be higher than ones driven by eastern wind. Respectively, the significant wave heights of East Taihu appear to be lower than other lake areas', it could be the result of narrow shape of bathmetry of East Taihu.

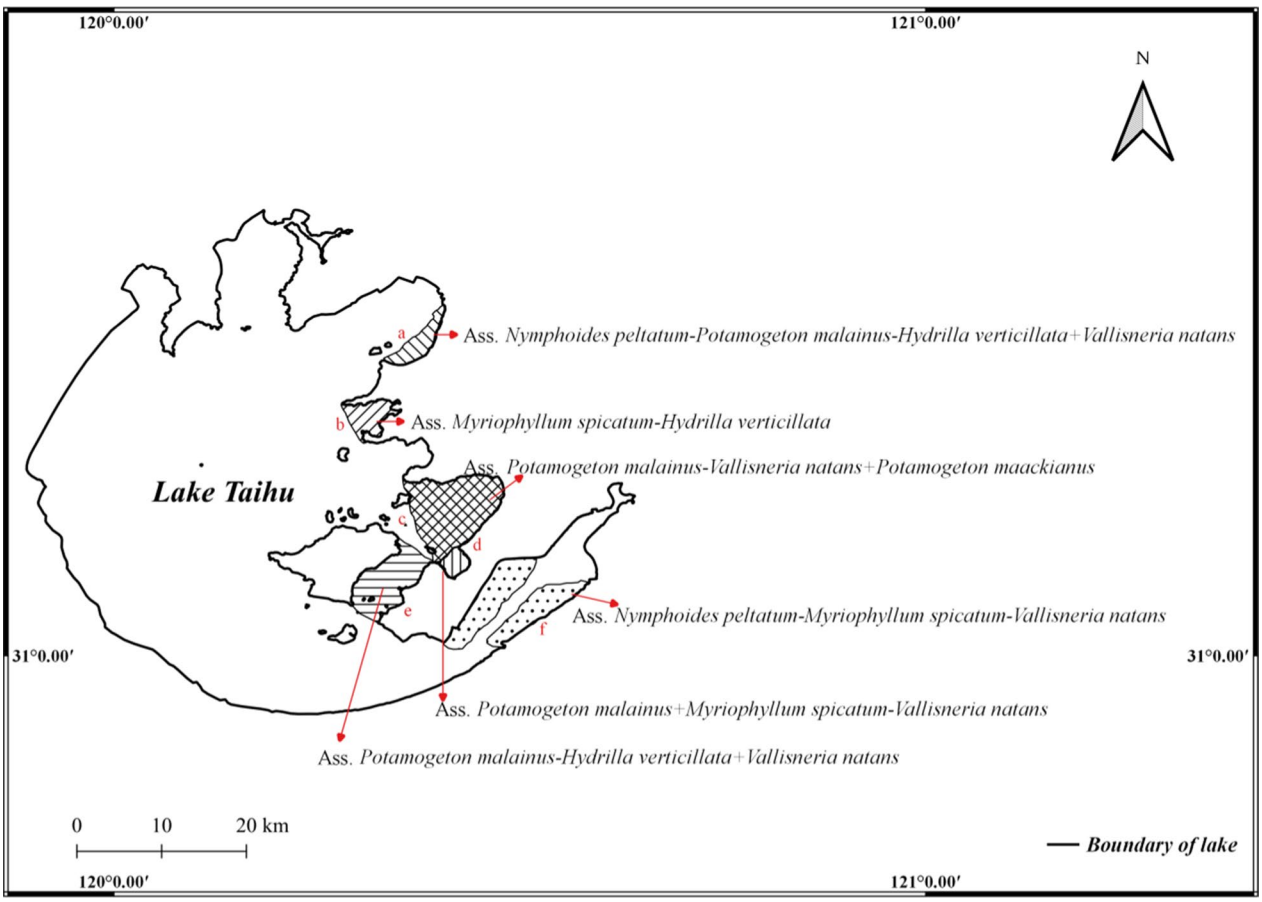

Fig. 3 Aquatic macrophyte associations classification in different lake area. In which, *a* represents Gonghu Bay, *b* represents Zhenhu Bay, *c* represents Xuhu Bay, *d* represents Xiaobai Lake, *e* represents Area between Xishan and Dongshan, *f* represents East Taihu

Table 1 Results of empirical formula and model simulation

	By Putian formula (m)				By MIKE 21 SW (m)			
Wind	**North**	**East**	**South**	**West**	**North**	**East**	**South**	**West**
CL1	0.191	0.225	0.179	0.178	0.199	0.230	0.184	0.182
CL2	0.201	0.200	0.216	0.195	0.208	0.200	0.233	0.197
CL3	0.222	0.163	0.151	0.164	0.225	0.162	0.142	0.159
CL4	0.181	0.199	0.212	0.172	0.191	0.202	0.221	0.191
CL5	0.171	0.172	0.185	0.185	0.172	0.173	0.196	0.191

Table 2 Statistical and uncertainty analysis of models established

	Nikuradse roughness (m)	R.bias	RMSE (m)
North	0.020	0.0299	0.0069
East	0.015	0.0107	0.0026
South	0.018	0.0529	0.0110
West	0.020	0.0390	0.0093

Wave attenuation caused by aquatic macrophyte

The vegetation-induced wave attenuation and changes in flow patterns had been observed and confirmed in prior research [34–46]. The attenuation in significant wave height for different vegetation drag coefficients within sampling line driven by both eastern and western wind conditions were investigated, respectively. By Eq. (12), the wave height attenuation rates are listed in Table 4 and 5, respectively.

Table 3 Simulation of significant wave heights driven by constant winds

Lake area	Sampling line	Length (km)	Significant wave heights (m)			
			North	East	South	West
Gonghu Bay	GH2	3.107	0.052–0.114	0.003–0.035	0.027–0.083	0.067–0.119
	GH3	4.045	0.049–0.113	0.018–0.071	0.001–0.047	0.049–0.096
Zhenhu Bay	ZH1	2.613	0.001–0.045	0.025–0.046	0.066–0.090	0.064–0.127
	ZH2	1.638	0.008–0.020	0.001–0.002	0.018–0.041	0.081–0.090
Xuhu Bay	XH1	5.808	0.038–0.074	0.011–0.074	0.021–0.083	0.047–0.100
	XH2	4.499	0.003–0.076	0.080–0.029	0.038–0.071	0.037–0.081
East Taihu	EC2	4.446	0.025–0.056	0.027–0.055	0.046–0.068	0.013–0.060
	EC3	4.256	0.027–0.051	0.010–0.039	0.004–0.030	0.037–0.052
	EC4	3.500	0.003–0.033	0.040–0.052	0.030–0.053	0.034–0.054

Table 4 Wave height attenuation rate ranges driven by eastern wind %

Lake area	Sampling line	Wave height attenuation		
		$C_D = 0.1$	$C_D = 0.2$	$C_D = 0.3$
Gonghu Bay	GH2	1.72–8.89	1.72–8.89	1.72–8.89
	GH3	0.52–3.18	0.52–3.18	0.52–3.18
Zhenhu Bay	ZH1	− 0.07 to 1.57	− 0.07 to 1.57	− 0.07 to 1.57
	ZH2	− 0.19 to 0.63	− 0.19 to 0.63	− 0.19 to 0.63
Xuhu Bay	XH1	0.34–7.61	0.34–7.61	0.34–7.61
	XH2	0.43–7.29	0.43–7.29	0.43–7.29
East Taihu	EC2	1.72–2.68	1.72–2.68	1.72–2.68
	EC3	− 0.03 to 0.46	− 0.03 to 0.46	− 0.03 to 0.46
	EC4	0.73–1.13	0.73–1.13	0.73–1.13

Table 5 Wave height attenuation rate ranges driven by western wind %

Lake area	Sampling line	Wave attenuation		
		$C_D = 0.1$	$C_D = 0.2$	$C_D = 0.3$
Gonghu Bay	GH2	0.03–0.32	0.03–0.32	0.03–0.32
	GH3	0.01–0.60	0.01–0.60	0.01–0.60
Zhenhu Bay	ZH1	0.41–1.20	0.43–1.20	0.43–1.20
	ZH2	7.59–8.30	7.78–8.65	7.78–8.65
Xuhu Bay	XH1	8.59–22.58	8.56–22.58	8.56–22.58
	XH2	9.20–23.37	9.18–23.37	9.18–23.37
East Taihu	EC2	0.02–3.31	0.02–3.31	0.02–3.31
	EC3	− 0.06 to 0.17	− 0.06 to 0.17	− 0.06 to 0.17
	EC4	− 0.08 to 0.55	− 0.08 to 0.55	− 0.08 to 0.55

Table 6 Results of delimitation of 26 sampling lines

Lake area	Sampling line	Length of sampling line (km)	Result of delimitation (m)
Gonghu Bay	GH1	6.099	1321
	GH2	3.134	1290–1309
	GH3	3.975	2093–2109
	GH4	3.792	1502
Zhenhu Bay	ZH1	2.613	1114–1124
	ZH2	1.638	1097–1120
Guangfu Bay	GF1	2.172	951–964
	GF2	2.500	1660–1690
Xuhu Bay	XH1	4.499	1527
	XH2	4.321	1853
East Taihu	EC1	3.014	1818
	EC2	4.446	1591–1707
	EC3	4.310	2138–2155
	EC4	3.500	1120
South Taihu	SC1	6.126	801–862
	SC2	5.821	1387–1433
	SC3	2.166	772–820
West Taihu	WC1	6.924	1017–1045
	WC2	6.868	1974–2001
Zhushan Bay	ZS1	2.776	720
	ZS2	3.116	701–726
	ZS3	3.653	1112
	ZS4	2.934	991
Meiliang Bay	ML1	4.879	1478–1575
	ML2	3.547	2141
	ML3	3.495	827–876

Delimitation results of radiant belt toward lake

Based on setups of sampling lines and sampling points, along with the mathematical expressions, in total of 26 sampling lines located in all lake areas of Lake Taihu were delimited, as shown in Table 6.

A total of 26 sampling lines were delimited, ranging 701–2155 m. Hereby, based on the setups of all sampling lines, the radiant belt toward lake of Lake Taihu ranges about 1–2 km.

Discussion

Statistical and uncertainty analysis of models established

Putian formula is an empirical formula based on long-term wind waves observation data, presented as a common method of wind waves calculation in China. R.bias and RMSE can be used to evaluate the accuracy of models established, the smaller the values are, the more accurate the models established. With an average R.bias at 0.0331 and an average RMSE at 0.0075 m, shows that the simulated wave heights are very close to computational results from Putian formula, which indicates that MIKE21 SW can simulate well in wave activities of Lake Taihu. Moreover, as listed in Table 1, the values simulated by MIKE21 SW are always slightly higher than ones by Putian formula, the same phenomenon were observed in similar research, as well [21, 47]. Hereby, it could be inferred as the computational biases caused by grid dissections of wave models. Nevertheless, the established models could be considered as accurate.

Wave height attenuation caused by aquatic macrophyte

Numerical simulation has enabled a large scope into wave height attenuation caused by aquatic macrophyte. In prior studies, the vegetation incorporated waves can be simulated in 2 approaches: (i) by corresponding modules developed by original softwares, i.e., SWAN-VEG [32], Xbeach-VEG [48] (ii) by introducing terms into governing equations of energy dissipation due to vegetation [49, 50]. However, MIKE21 SW was rarely applied as a result of lacks in corresponding modules. Gui [51] pointed out that bottom friction could be increased as a result of presence of vegetation on lake bed. Hereby, combining field survey and mathematical formula, this research has developed a proper approach coupling aquatic macrophyte into wave models via MIKE21 SW.

Currently, aquatic vegetation on lake bed are treated as idealized cylinders in numerical simulation [52], which leads to a good agreement in rigid aquatic vegetation [53]. By introducing concession factor D in C_D to simulate the swaying of flexible vegetation, the agreement between experimental and simulation data were improved in SWAN-VEG [53]. With reference to Oude's research [32], the C_D was properly decreased to 0.1 ~ 0.3. The wave attenuation rate ranges from −0.19% ~ 8.89% by eastern wind, and −0.08% ~ 23.37% by western wind, indicating the very need of aquatic vegetation incorporation. However, the minimum attenuation rate −0.19% (in ZH2 eastern wind) indicates a slight increase in wave height, it is probably because that energy accumulation happening at some sampling point. In consider of the original simulation results in ZH2 (0.001 m–0.002 m), it could be the computational biases as the result of the small wave height, as well. Little of research had considered a large scale of vegetated-wave in numerical simulation [32]. In addition, the flow regime and species, rigidity and composition of aquatic vegetation were different case by case [32]. Hence, with an average attenuation rate of 4.95% driven by western wind, and ones driven by eastern wind is 2.17%, the wave height attenuation rate could be considered as appropriate.

The wave height attenuation is related to wave parameters and vegetation characteristics [35]. In Tables 4 and 5, the changes in wave height attenuation were observed as a result of changes in wind directions. Longer fetch makes it possible for wave grow adequately, thus a higher attenuation rate, similar conclusions were drawn out in Paquier's [54] and Reidenbach's [55] research, as well. By changing C_D, the wave height attenuation appears slight change. Similar results were found in Gui's [51] study of parameter analysis in MIKE21 SW, when bottom friction increase to some specific value, the wave attenuation stops changing. Hereby, it could be inferred as a fully attenuation happened in present research. Smaller wave heights make it insignificant in wave height attenuation calculation process.

Delimitation of radiant belt toward lake

According to definition of radiant belt toward lake, the boundary of it is the end point of terrestrial impact on water area. With reference to coastal zone, abrupt change point of relative wave height was used to delimit the boundary. It was found in each sampling line of all lake areas. Exampled by GH1 (Fig. 4a), changes in wind forcing have shown slight impact on the abrupt change point (point 110 in GH1), same phenomena were observed at all other sampling lines. Changes in delimitation result were at most 116 m (in EC2) when wind direction changes. It can be recognized reasonable in consider of the large scale of Lake Taihu. As it is listed in Table 5, the curves of XH2 (Fig. 4b) whose wave attenuation is the highest are found the presence of aquatic macrophyte show no impact on the abrupt change point (point 225 in XH2). The delimitation results are barely influenced when wind and aquatic macrophyte parameters change. Hence, a novel approach has been developed

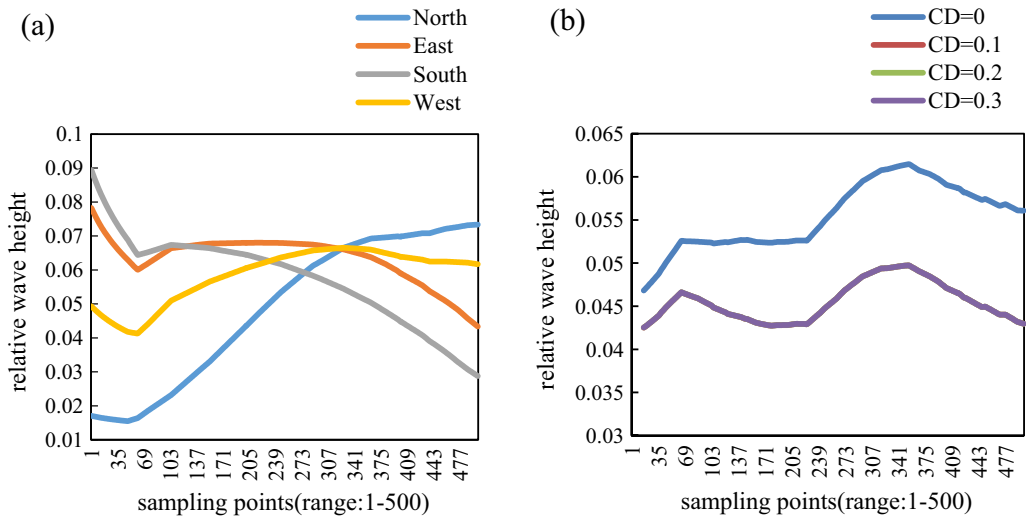

Fig. 4 **a** Delimitation of GH1 by different wind forcing. **b** Delimitation of XH2 by western wind

for quantitative delimit radiant belt toward lake of Lake Taihu. The result of delimitation could provide a theoretical boundary for lake-terrestrial ecotone for more precise protection and restoration. Moreover, the approach this research developed could also provide a proper way to quantitative delimit for large shallow lakes with similar conditions, as well.

Conclusions

A novel approach was developed to quantitatively delimit the range of radiant belt toward lake of Lake Taihu from wave perspective via numerical simulation. According to the definition, aquatic macrophyte obtained by field survey were incorporated into wave models. As a result, the wave height attenuation was observed in present work. Based on the setups of sampling line and delimitation result, the range of radiant belt toward lake was identified as 1 ~ 2 km. The boundary this research delimit could provide a theoretical basis for more precise lake-terrestrial ecotone protection and restoration for Lake Taihu. Moreover, the approach this research developed could provide a method for quantitative delimitation of large shallow lake with similar conditions, as well.

Abbreviations

MSWT: Moving split-window technology; IV: Important value; RMSE: Root mean square error; C_D: Vegetation drag coefficient.

Supplementary Information

The online version contains supplementary material available at https://doi.org/10.1186/s12302-022-00615-1.

Additional file 1. Schematic of field survey.

Additional file 2. Schematic of Equivalent fetch length.

Additional file 3. Important value of aquatic macrophyte.

Additional file 4. The parameters obtained in field survey.

Additional file 5. Coordinates of calibration point.

Acknowledgements

We would like to thank Yang Wang, Wen Hu and Yun Chen for their help in field survey July, 2021. We also would like to thank Dr. Zi-jian Xie, Dr. Qi Zhu for their advice on original manuscript. Besides, we would like to thank Hao Wang, Yi-xue Xu and Ye Zheng for their kind help during the process of this research.

Authors' contributions

TYC: conceptualization, methodology, formal analysis, investigation, and writing—original draft; CY: validation, resources, writing—review and editing, and supervision; CHL: validation, resources, writing—review and editing, and supervision; FZ: validation, resources, and writing—review and editing; WWW: investigation. All authors read and approved the final manuscript.

Funding

This research was jointly supported by National Key Research and Development Program of China (2021YFC3201504) "Watershed non-point source pollution prevention and control technology and application demonstration" and Transformation and Promotion of Ecological Space Management and Control Technology, China (No. 2020-JY-018).

Availability of data and materials

The data sets used and/or analyzed during the current study are available from the corresponding author on reasonable request.

Declarations

Ethics approval and consent to participate
Not applicable.

Consent for publication
Not applicable.

Competing interests
The authors declare that they have no competing interests.

Received: 20 January 2022 Accepted: 22 March 2022
Published online: 15 April 2022

References

1. Ye C, Li C, Deng T (2015) Structures and ecological functions of lake littoral zones. Res Environ Sci 28:171–181. https://doi.org/10.13198/j.issn.1001-6929.2015.02.02 (**In Chinese**)
2. Zheng P, Shang X, Ye C, Li C, Zheng X, Dai W, Wei W (2021) Delimiting the radiant belt toward land of lake-terrestrial ecotone with natural-wetland type. Res Environ Sci 34:953–963. https://doi.org/10.13198/j.issn.1001-6929.2020.12.29 (**In Chinese**)
3. Kalff J (2002) Limnology: inland water ecosystems. Prentice-Hall, New Jersey
4. Zhao D, Hao J, Yang T, Cai Y, Xu D, An S (2012) Remote sensing of aquatic vegetation distribution in Taihu Lake using an improved classification tree with modified thresholds. J Environ Manage 95(1):98–107. https://doi.org/10.1016/j.jenvman.2011.10.007
5. Wang S, Gao Y, Li Q, Gao J, Zhai S, Zhou Y, Cheng Y (2018) Long-term and inter-monthly dynamics of aquatic vegetation and its relationship with environmental factors in Taihu Lake, China. Sci Total Environ 651:367–380. https://doi.org/10.1016/j.scitotenv.2018.09.216
6. Kimiaghalam N, Clark S, Ahmari H, Hunt J (2015) Wave-current induced erosion of cohesive riverbanks in northern Manitoba, Canada. Proc Int Assoc Hydrol Sci 367:134–140. https://doi.org/10.5194/piahs-367-134-2015
7. Brenninkmeyer BM (1982) Wave erosion. In: Beaches and Coastal Geology. Encyclopedia of Earth Sciences Series. Springer, New York, NY. https://doi.org/10.1007/0-387-30843-1_492.
8. Tang C, Li Y, He C, Acharya K (2020) Dynamic behavior of sediment resuspension and nutrients release in the shallow and wind exposed Meiliang Bay of Lake Taihu. Sci Total Environ 708:135131.1-135131.10. https://doi.org/10.1016/j.scitotenv.2019.135131
9. Rodriguez A, Sánchez-Arcilla A, Redondo JM, Ahia EB, Sierra JP (1995) Pollutant dispersion in the nearshore region: modelling and measurements. Water Sci Technol 32(9–10):169–178. https://doi.org/10.1016/0273-1223(96)00088-1
10. Herbich JB, Haney JP (1982) Coastal engineering. In: Beaches and Coastal Geology. Encyclopedia of Earth Sciences Series. Springer, New York, NY. https://doi.org/10.1007/0-387-30843-1_111.
11. Marsooli R, Wu W (2014) Numerical investigation of wave attenuation by vegetation using a 3D RANS model. Adv Water Resour 74:245–257. https://doi.org/10.1016/j.advwatres.2014.09.012
12. Arunakumar HS, Suvarna P, Abhijith PA, Prabhu AS, Kamath A (2019) Effect of emerged coastal vegetation on wave attenuation using open source CFD tool: REEF3D. Proceedings of the Fourth International Conference in Ocean Engineering (ICOE2018), pp 591–603. https://doi.org/10.1007/978-981-13-3119-0_37.
13. Xiang Y, Fu SY, Zhu K, Yuan H, Fang ZY (2017) Seepage safety monitoring model for an earth rock dam under influence of high-impact typhoons based on particle swarm optimization algorithm. Water Sci Eng 10:70–77. https://doi.org/10.1016/j.wse.2017.03.005
14. Mentaschi L, Besio G, Cassola F, Mazzino A (2015) Performance evaluation of WAVEWATCH III in the Mediterranean Sea. Ocean Model 90:82–94. https://doi.org/10.1016/j.ocemod.2015.04.003
15. Lee HS (2015) Evaluation of WAVEWATCH III performance with wind input and dissipation source terms using wave buoy measurements for October 2006 along the east Korean coast in the East Sea. Ocean Eng 100:67–82. https://doi.org/10.1016/j.oceaneng.2015.03.009
16. Longodan S, Cavaleri L, Viswanahapalli Y, Hoteit I (2014) The Red Sea: a natural laboratory for wing and wave modelling. J Phys Oceanogr 44:4139–3159
17. Seemanth M, Bhowmick SA, Kumar R, Sharma R (2016) Sensitivity analysis of dissipation parameterizations in a third-generation spectral wave model, WAVEWATCH III for Indian Ocean. Ocean Eng 127:252–273. https://doi.org/10.1016/j.oceaneng.2016.07.023
18. Akpinar A, Vledder GV, Komurcu MI, Ozger M (2012) Evaluation of the numerical wave model (SWAN) for wave simulation in the Black Sea. Cont Shelf Res 50:80–89. https://doi.org/10.1016/j.csr.2012.09.012
19. Wolf J, Hargreaves JC, Flather RA (2000) Application of the SWAN shallow water wave model to some UK coastal sites. Proudman Oceanographic Laboratory.
20. Li Y, Pang Y, Liu X, Luo L, Xu Q (2008) Numerical modelling of waves in Lake Taihu. J Lake Sci 20:117–122. https://doi.org/10.18307/2008.0118 (**In Chinese**)
21. Zhao J, Li J (2017) Numerical simulation of wind waves in Taihu Lake. J Water Resourc Archit Eng. 15:204–209. https://doi.org/10.3969/j.issn.1672-1144.2017.01.039(**In Chinese**)
22. Fonseca RB, Goncalves M, GuedesSoares C (2017) Comparing the performance of spectral wave models for coastal areas. J Coast Res 33:331–346. https://doi.org/10.2112/JCOASTRES-D-15-00200.1
23. Gao HL, Cheng HF, Zhan MH, Wang BY (2019) Research progress of aquatic macrophytes in Taihu Lake. Wetland Sci 17:9–15. https://doi.org/10.13248/j.cnki.wetlandsci.2019.01.002 (**In Chinese**)
24. Danish Hydraulic Institute (DHI) (2015) MIKE 21 SW Reference Manual, MIKE by DHI, Manual Mesh Generator; MIKE Zero: Hørsholm, Denmark.
25. Chinese Code for design of levee project (GB50286–2013) (2013)
26. Jiang B, Yang K, Cao S, Chen L (2012) Modeling the velocity distribution in compound channels with vegetated floodplains based on the equivalent resistance. J Hydraul Eng 43:20–26. https://doi.org/10.13243/j.cnki.slxb.2012.s2.023 (**In Chinese**)
27. Zhang M, Shen Y, Zhu L (2008) Depth-averaged two-dimensional numerical simulation for curved open channels with vegetation. J Hydraul Eng 39:794–800. https://doi.org/10.13243/j.cnki.slxb.2008.07.007 (**In Chinese**)
28. Tang H, Yan J, Xiao Y, Lu S (2007) Manning's roughness coefficient of vegetated channels. J Hydraul Eng 38:1347–1353. https://doi.org/10.13243/j.cnki.slxb.2007.11.018 (**In Chinese**)
29. Xu T, Zhang M, Jiang H, Tang J, Zhang H, Qiao H (2019) Numerical investigation of the effects of aquatic plants on wind-induced currents in Taihu Lake in China. J Hydrodyn 31:778–787. https://doi.org/10.1007/s42241-018-0091-9
30. Hemavathi S, Manjula R (2020) Wave attenuation by heterospecific coastal vegetation-modelling through response surface methodology on synthetic plant meadows. Curr Sci 119:497–506. https://doi.org/10.18520/cs/v119/i3/497-506
31. Houser C, Trimble S, Morales B (2015) Influence of blade flexibility on the drag coefficient of aquatic vegetation. Estuar Coast 38:569–577. https://doi.org/10.1007/s12237-014-9840-3
32. Oude R. de (2010) Modelling wave attenuation by vegetation with SWAN-VEG: Model evaluation and application to the Noordwaard polder. MS thesis. University of Twente.
33. Qin B, Hu W, Chen W (2004) Processes and mechanisms of water environment evolution in Taihu Lake. Science Press, Beijing (**In Chinese**)
34. Dalrymple RA, Kirby JT, Hwang PA (1984) Wave diffraction due to areas of energy dissipation. J Waterw Port Coast Ocean Eng 110:67–79. https://doi.org/10.1061/(ASCE)0733-950X(1984)110:1(67)
35. Mendez FM, Losada IJ (2004) An empirical model to estimate the propagation of random breaking and non-breaking waves over vegetation fields. Coast Eng 51:103–118. https://doi.org/10.1016/j.coastaleng.2003.11.003
36. Bradley K, Houser C (2009) Relative velocity of seagrass blades: implications for wave attenuation in low-energy environments. J Geophys Res Earth Surf 114(F1):1–13. https://doi.org/10.1029/2007JF000951
37. Paul M, Amos CL (2011) Spatial and seasonal variation in wave attenuation over *Zostera noltii*. J Geophys Res Oceans 116(C8):1–16. https://doi.org/10.1029/2010JC006797

38. Kobayashi N, Raichle AW, Asano T (1993) Wave attenuation by vegetation. J Waterw Port Coast Ocean Eng 119(1):30–48. https://doi.org/10.1061/(ASCE)0733-950X(1993)119:1(30)
39. Maza M, Lara JL, Losada IJ (2013) A coupled model of submerged vegetation under oscillatory flow using Navier Strokes equations. Coast Eng 80(7):16–34. https://doi.org/10.1016/j.coastaleng.2013.04.009
40. Koftis T, Prinos P, Stratigaki V (2013) Wave damping over artificial Posidonia oceanica meadow: a large-scale experimental study. Coast Eng 73(3):71–83. https://doi.org/10.1016/j.coastaleng.2012.10.007
41. Lopez F, Garci AMH (2001) Mean flow and turbulence structure of open-channel flow through non-emergent vegetation. J Hydraul Eng 127(5):392–402. https://doi.org/10.1061/(ASCE)0733-9429(2001)127:5(392)
42. Wilson C, Pinzen AB, Bates PD, Stoesser T (2006) Open channel flow through different forms of submerged flexible vegetation. J Hydraul Eng 129(11):750. https://doi.org/10.1061/(ASCE)0733-9429(2003)129:11(847)
43. Huai W, Han J, Geng C, Zhou J, Zeng Y (2010) The mechanism of energy loss and transition in a flow with submerged vegetation. Adv Water Resour 33(6):635–639. https://doi.org/10.1016/j.advwatres.2010.03.006
44. Knutson PL, Brochu RA, Seelig WN, Inskeep M (1982) Wave damping in *Spartina alterniflora* marshed. Wetlands 2:87–104. https://doi.org/10.1007/BF03160548
45. Tanino Y, Nepf HM (2008) Laboratory investigation of mean drag in a random array of rigid, emergent cylinders. J Hydraul Eng 134(1):34–41. https://doi.org/10.1061/(ASCE)0733-9429(2008)134:1(34)
46. Fathi-Maghadam M, Kouwen N (1997) Non-rigid, non-submerged, vegetative roughness on floodplains. J Hydraul Eng 123(1):51–57. https://doi.org/10.1061/(ASCE)0733-9429(1997)123:1(51)
47. Xiang Y, Fu Z, Meng Y, Zhang K, Cheng Z (2019) Analysis of wave clipping effects of plain reservoir artificial islands based on MIKE21 SW model. Water Sci Eng 12(3):179–187. https://doi.org/10.1016/j.wse.2019.08.002
48. Figueroa-Alfaro RW, Van Rooijen A, Garzon JL, Evans M, Harris A (2022) Modelling wave attenuation by saltmarsh using satellite-derived vegetation properties. Ecol Eng 176:106528. https://doi.org/10.1016/j.ecoleng.2021.106528
49. Dubi A, Tørum A (1995) Wave damping by kelp vegetation. In Coastal Engineering 1994 (pp.142–156). https://doi.org/10.1061/9780784400890.012
50. Tang J, Causon D, Mingham C, Qian L (2013) Numerical study of vegetation damping effects on solitary wave run-up using the nonlinear shallow water equations. Coast Eng 75:21–28. https://doi.org/10.1016/j.coastaleng.2013.01.002
51. Gui J, Feng M., Zhang R (2014) Explore the Influence of Bottom Friction Parameter and Wave Breaking Parameter on Wave Height and Wave Period by MIKE21 SW Module. In Applied Mechanics and Materials (Vol. 501, pp. 2124–2127). Trans Tech Publications Ltd. https://doi.org/10.4028/www.scientific.net/AMM.501-504.2124
52. Stoesser T, Kim SJ, Diplas P (2010) Turbulent flow through idealized emergent vegetation. J Hydraul Eng 136:1003–1017. https://doi.org/10.1061/(ASCE)HY.1943-7900.0000153
53. Cao H, Feng W, Li J (2013) Research on the modelling of the wave attenuation due to vegetation based on SWAN-VEG. Sci Technol Eng 13:2430–2436. https://doi.org/10.3969/j.issn.1671-1815.2013.09.023 (**In Chinese**)
54. Paquier AE, Meulé S, Anthony EJ, Larroudé P, Bernard G (2019) Wind-induced hydrodynamic interactions with aquatic vegetation in a fetch-limited setting: implications for coastal sedimentation and protection. Estuar Coast 42:688–707. https://doi.org/10.1007/s12237-018-00487-w
55. Reidenbach MA, Thomas EL (2018) Influence of the Seagrass, *Zostera marina*, on wave attenuation and bed shear stress within a shallow coastal bay. Front Mar Sci 5:397. https://doi.org/10.3389/fmars.2018.00397

Publisher's Note